Available online at www.sciencedirect.com
ScienceDirect
Bioorganic & Medicinal Chemistry 15 (2007) 1848–1858
Bioorganic & Medicinal Chemistry

Specific interactions with intra- and intermolecular G-quadruplex DNA structures by hydrosoluble coronene derivatives: A new class of telomerase inhibitors

Marco Franceschin,[a,*] Antonello Alvino,[a] Valentina Casagrande,[a] Clementina Mauriello,[b] Emanuela Pascucci,[b] Maria Savino,[b,c] Giancarlo Ortaggi[a] and Armandodoriano Bianco[a,d]

[a]*Dipartimento di Chimica, Università di Roma 'La Sapienza', Piazzale A. Moro 5, 00185 Roma, Italy*
[b]*Dipartimento di Genetica e Biologia Molecolare, Università di Roma 'La Sapienza', Piazzale A. Moro 5, 00185 Roma, Italy*
[c]*Istituto di Biologia e Patologia Molecolare del CNR, Università di Roma 'La Sapienza', Piazzale A. Moro 5, 00185 Roma, Italy*
[d]*Istituto di Chimica Biomolecolare del CNR, Università di Roma 'La Sapienza', Piazzale A. Moro 5, 00185 Roma, Italy*

Received 18 July 2006; revised 10 November 2006; accepted 17 November 2006
Available online 19 November 2006

Abstract—In developing G-quadruplex interactive telomerase inhibitors two main features have to be taken into account: the hydrophobic interactions with the G-quartet plane and the electrostatic interactions with the negatively charged phosphates of the four grooves. In this paper, we report the synthesis of four hydrosoluble coronene derivatives, which are characterized by a large hydrophobic aromatic core and four orthogonal hydrophilic side chains. We have studied their ability to induce both inter- and intramolecular G-quadruplex structures and found a significant selectivity of all the coronene derivatives for the intramolecular G-quadruplex. The efficiency in inhibiting human telomerase has been evaluated in a cell-free system and the experimental results correlate with the relative affinities of these compounds for the G-quadruplex monomeric structure, as derived by molecular modelling simulations. Thus, the coronene derivatives can be considered as a new class of telomerase inhibitors, although further investigations are surely necessary to fully exploit their features.
© 2006 Elsevier Ltd. All rights reserved.

1. Introduction

G-quadruplexes are unusual DNA secondary structures based on planes consisting of four guanines (G-tetrads) stabilized by Hoogsteen G–G pairings and monovalent cations[1] (Fig. 1). Although based on the same central moiety, many different G-quadruplex structures can arise depending on the number of strands and their orientation, leading to different loops and grooves.[2] These structures are particularly important for naturally occurring G-rich sequences, such as those present at the end of eukaryotic chromosomes (telomeres).[3] Moreover, the presence in the cell of proteins that bind and/or induce G-quadruplexes,[4] as well as helicases able to unwind specifically these structures,[5] suggests that G-quadruplexes represent biologically important signalling structures. Recent evidence of the existence of G-quadruplex structures in vivo supports this hypothesis.[6,7]

Classical G-quadruplex ligands present an aromatic core suitable for π–π stacking interactions with the terminal G-tetrad of a DNA G-quadruplex, while the hydrophilic side chains interact with the DNA grooves.[8] These compounds are able to inhibit human telomerase, since the enzyme is not able to bind to its substrate (the telomere) if it is firmly folded in a G-quadruplex structure.[9] Since telomerase is not active in most somatic cells but is active in most human tumours, telomere targeting and telomerase inhibition have gained great consideration for new highly selective anti-tumour strategies.[10] A wide range of such small molecules have been characterized, including acridines,[11] triazines,[12] porphyrins,[13] perylenes[14] and berberine derivatives.[15]

We have previously reported the synthesis of a new hydrosoluble coronene derivative (CORON, Fig. 2) with four polar side chains containing piperidine.[16]

Keywords: Hydrosoluble coronene derivatives; G-quadruplex; Telomerase inhibitors.
* Corresponding author. Tel.: +39 0649913341; fax: +39 064462778; e-mail: marco.franceschin@uniroma1.it

0968-0896/$ - see front matter © 2006 Elsevier Ltd. All rights reserved.
doi:10.1016/j.bmc.2006.11.032

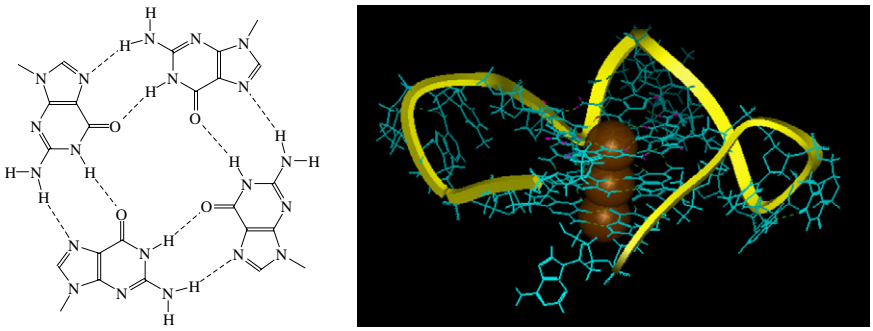

Figure 1. Schematic representation of a G-tetrad (left). The X-ray-derived monomeric structure[18] of the 22-mer human telomeric DNA sequence $AGGG(TTAGGG)_3$ used in the molecular modelling simulations (right): the yellow ribbon indicates the strand topology, the K^+ ions are in orange, the H-bonds in green and the binding site used for the docking in violet.

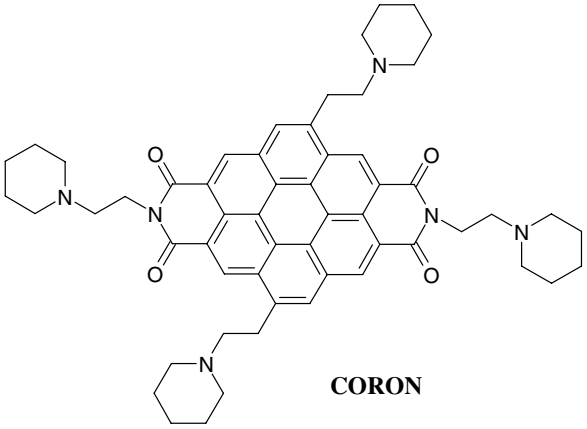

Figure 2.

The simultaneous presence of a large hydrophobic core and four flexible hydrophilic chains gives rise to very interesting physico-chemical properties: this compound is soluble in organic solvents in the basic form and in aqueous solution as a hydrochloride. These two molecular features are essential in determining the interactions between this molecule and G-quadruplex DNA structures. Our previous studies on perylene diimides[14] showed that the polar side chains play a major role in determining the ability of these compounds to bind to the G-quadruplex. In particular, the highest efficiency in inducing G-quadruplex structures and inhibiting telomerase was obtained for the compounds with piperazino-ethyl and dimethylamino-propyl side chains, rather than for the original piperidino-ethyl containing PIPER.[17] In this work, we report the synthesis of three new coronene derivatives (Fig. 3), using side chains similar to those which led to the best biological activity in the perylene series, and a study of their interactions with G-quadruplex structures and their ability to inhibit telomerase.

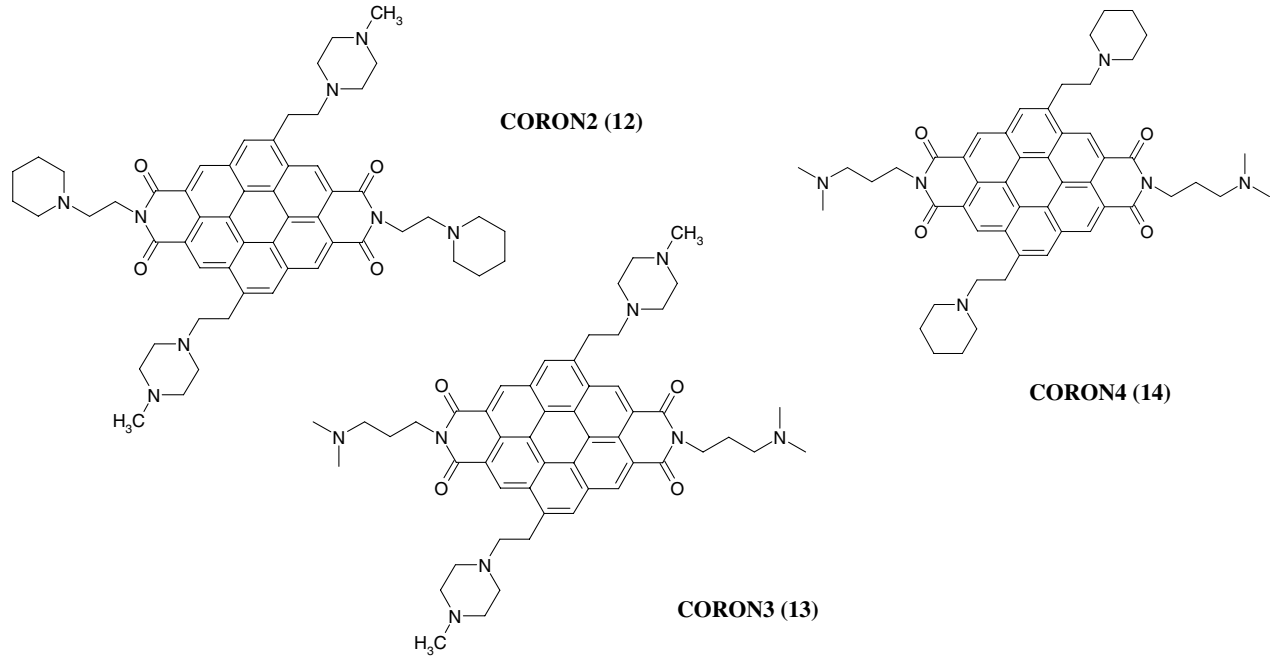

Figure 3. The new coronene derivatives.

2. Results and discussion

2.1. Molecular modelling

Simulated annealing of the previously reported CORON[16] (Fig. 1) on a G-quadruplex monomeric structure[18] was performed as described in Section 4. The resulting structure of the complex between G-quadruplex and CORON (Fig. 4A) shows a good superimposition of the large aromatic core of the ligand and the terminal G-tetrad of the G-quadruplex. The four side chains are correctly directed towards the four grooves of the G-quadruplex and at least two of them are well fitted into two adjacent grooves. This model confirms the 'threading intercalation' model for coronene derivatives, as has also been proposed for many G-quadruplex ligands.[19] When performing the same simulations on the other three derivatives, similar models were obtained (Fig. 4B). The interaction energies between the G-quadruplex and the ligand obtained for the four compounds are reported in Table 1. Due to the simplicity of the molecular modelling procedure used (in particular the rigidity of DNA and the absence of explicit water molecules) the binding energies must be considered in a relative order for this series of homologous compounds and not as absolute values. Moreover, it is worth noting that the parallel monomeric structure we used is only one of the many possible G-quadruplex structures.[20] Nevertheless, it has been widely used for molecular modelling[11,21] and, from the model we obtained using this specific structure, it is possible to note that the three new compounds are predicted to be more efficiently bound to the monomeric G-quadruplex than CORON. This is mainly due to the flexibility of the longer side chains (with a propyl linker instead of the

Table 1. Medium binding energies over 25 structures for the complexes between the human monomeric G-quadruplex structure and the specified ligand, derived by simulated annealing as described in Section 4

Ligand	Binding energy (kcal/mol)
CORON	−1889 ± 22
CORON2	−1915 ± 37
CORON3	−1941 ± 34
CORON4	−1918 ± 35

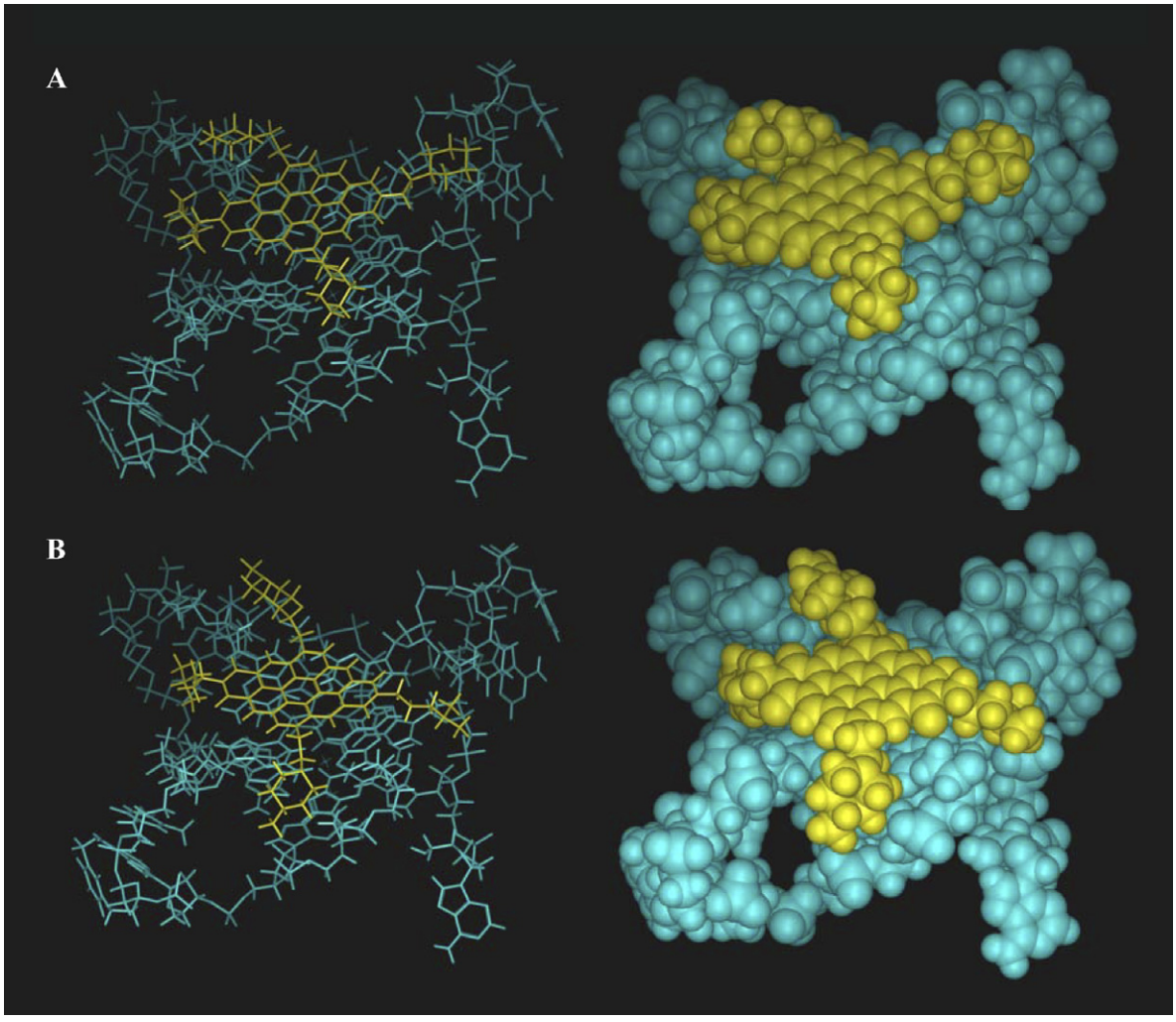

Figure 4. Complexes between coronene derivatives (yellow) and a monomeric G-quadruplex (blue) obtained by simulated annealing. Sticks and lines (left) and CPK model (right). (A) CORON (B) CORON3.

ethyl chain of CORON) and the presence of a larger number of basic nitrogen atoms of the piperazine ring with respect to the piperidine ring (Fig. 4B). This agrees with our previous results obtained in the series of perylene diimides.[14]

2.2. Chemical synthesis

The three new hydrosoluble coronene derivatives were synthesized using the same strategy we reported for the synthesis of CORON[16] (Scheme 1), previously

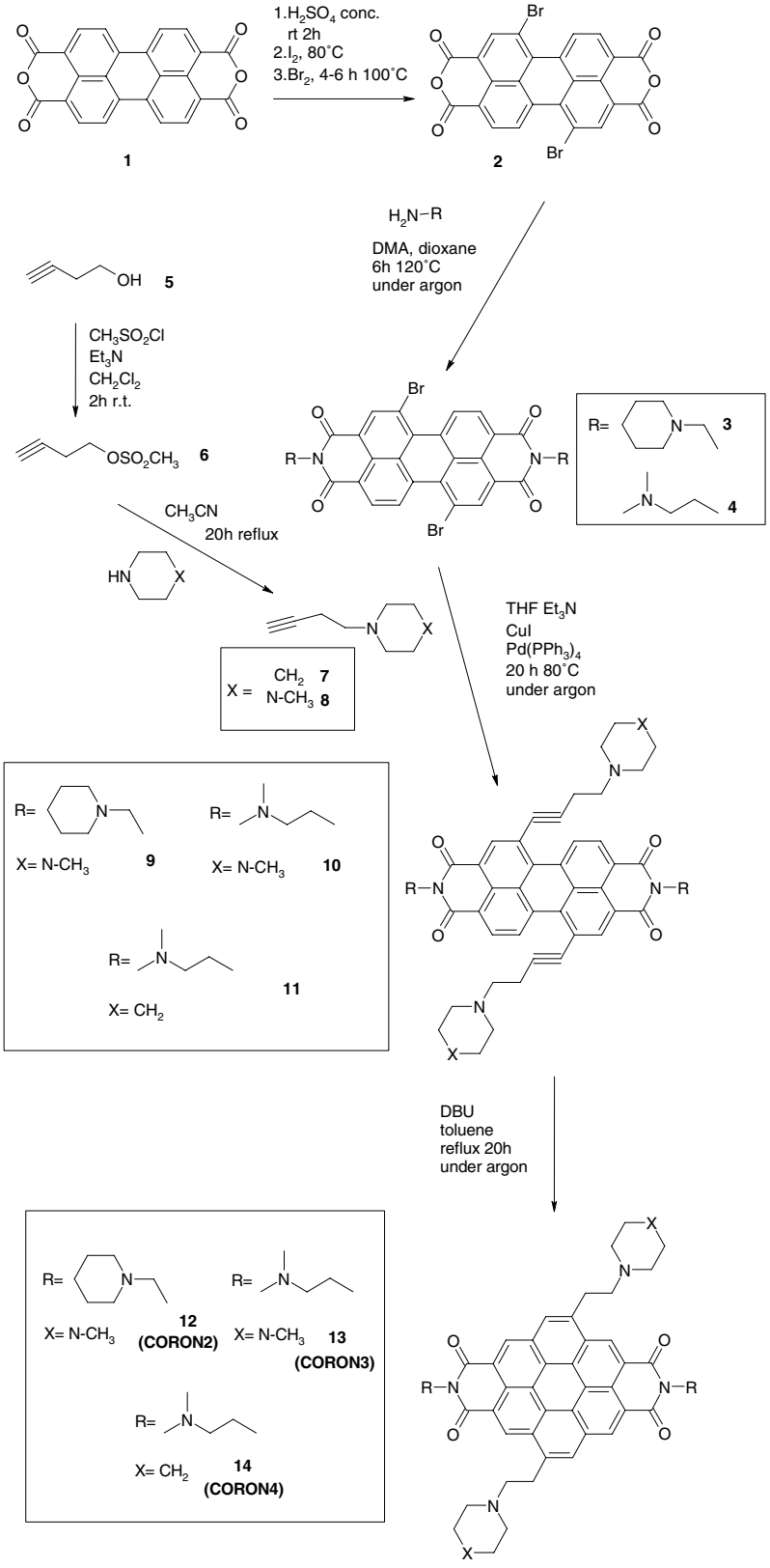

Scheme 1.

described by Mullen and co-workers for lipophilic derivatives.[22]

The first step of the synthetic strategy is the bromination of the bay area of 3,4:9,10-perylenetetracarboxylic dianhydride (**1**) to obtain two functionalized positions able to react in the subsequent steps. Four positions (1, 6, 7 and 11) of the perylene moiety are reactive, but electronic and steric reasons allow only two dibromo derivatives to be obtained, whose ratio is determined by the reaction conditions: the major isomer was always 1,7-dibromoperylene-3,4:9,10-tetracarboxylic dianhydride (**2**) and the minor one the corresponding 1,6-derivative. Temperature and reaction time have been shown to be key parameters in determining the ratio between the two isomers. In particular, keeping the temperature at 100 °C for 4–6 h, the highest amount of the major isomer was obtained, approximately in a 6:1 ratio with respect to the minor 1,6-isomer. A small amount of the 1,6-isomer was always present, as could be determined by analyzing the ^{1}H NMR spectra of **2**. In Scheme 1 only the isomer **2** and the relative subsequent products are shown.

The second step consists of the addition of the side chains on the major axis of the perylene core, by reaction of the anhydridic group with primary amines having opportunely functionalized chains, as we focused on perylene diimides.[14] In this way we obtained two different compounds: PIPER-Br (**3**) and DAPER-Br (**4**).

In order to proceed towards the formation of the coronene aromatic core, suitable functionalized alkynes were prepared, having 1-piperidine (**7**) or 1-(4-methyl)-piperazine (**8**) at the end of the linear chain. Compound **7** is the same alkyne used in the CORON synthesis to obtain the PIPER-like side chain. Compound **8** was used to obtain side chains similar to those of the perylene derivative showing the best biological activity, which contained piperazine.[14] Compounds **7** and **8** were purified in two different ways due to their different hydrosolubility.

These functionalized alkynes were successively used in the Sonogashira cross-coupling[22,23] to synthesize the intermediate compounds **9**, **10**, and **11**. This reaction is catalyzed by Pd(0) complexes in the presence of CuI and a suitable base, leading to a new C–C bond. If a secondary amine is used as a base, alternative substitution of the bromine atoms can occur.[16] This is the main reason for using methyl-piperazine (a tertiary amine) instead of piperazine in the preparation of the alkynes for the synthesis of compounds **9** and **10**. In the Sonogashira coupling, the cyclization described in the next step also partially occurs. Separation was not useful at this stage, so the mixtures of each intermediate compound and the related partially closed products were used in the following step.

In order to complete the coronene aromatic core, a base-catalyzed cyclization was performed with DBU.[22] It was necessary to avoid using a nucleophilic base, in order to prevent hydrolysis of the imide group. The compounds CORON2 (**12**), CORON3 (**13**) and CORON4 (**14**) were thus obtained and converted into the respective water-soluble hydrochlorides by precipitation with acetone from an acid aqueous solution (HCl).

2.3. Spectroscopic properties

Due to the presence of four polar side chains, the coronene derivatives are hydrosoluble as hydrochlorides. Nevertheless, the presence of a large central aromatic core favours stacking interactions between these molecules. It was not possible to predict the result of these two opposite molecular features on the molecular organization of these compounds in different solvents. It is evident from the appearance of the electronic spectra that the presence of the four hydrophilic side chains is not sufficient to overcome the tendency of self-aggregation by the large hydrophobic cores of the coronene moiety. This is shown by the features of the absorption spectra performed in MES–KCl buffer (pH 6.5) with respect to those obtained in DMSO. In fact, in organic solvents these molecules show the characteristic six bands of

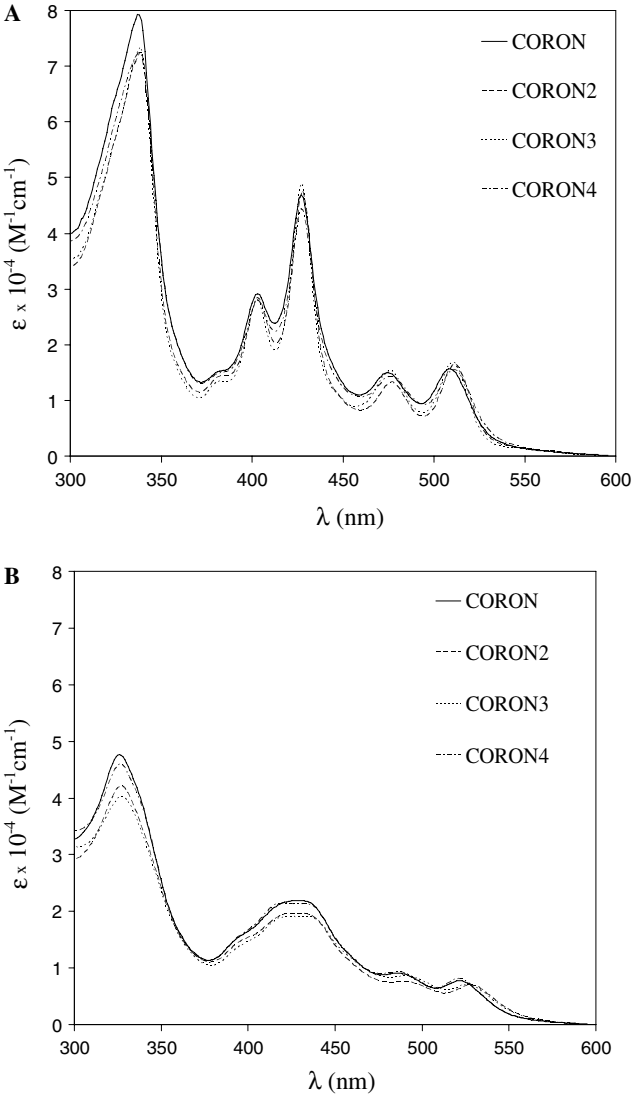

Figure 5. UV–vis absorption spectra of coronene derivatives in DMSO (A) and in MES–KCl aqueous buffer (pH 6.5) (B).

coronene,[22] while in aqueous solution a minor resolution of the bands and a remarkable hypochromic effect with respect to the spectra in DMSO can be observed (Fig. 5).

In order to analyze the stability of these aggregates, several experiments were performed. First spectra in MES–KCl buffer were obtained at different drug concentrations (from 10 to 40 μM) to study the effect of dilution on the extinction coefficients (Supplementary data, S1), but no significant change was detected, suggesting that the self-aggregation has no variation in this concentration range. Spectra in MES–KCl buffer were then performed at different temperatures (from 30 to 90 °C). The extinction coefficient variation was not very high, but it was possible to observe the emergence of a peak at 432 nm, from the low and broad band present in water solution between 417 and 438 nm (Supplementary data, S2). Finally, melting experiments were performed by registering the absorbance at a fixed wavelength while the temperature was slowly increased: an extinction coefficient percentage variation of about 13–23% was observed in the temperature range 30–90 °C (Supplementary data, S3).

These results confirmed the hypothesis of a self-aggregation process in aqueous solution for the coronene derivatives and suggested that these aggregates are very stable in the micromolar concentration range.

2.4. Inter- and intramolecular G-quadruplex DNA induction

The ability of the four hydrosoluble coronene derivatives to induce the formation of intra- and intermolecular G-quadruplex structures was investigated by PAGE (polyacrylamide gel electrophoresis).

The DNA oligonucleotides 2HTR and TSG4 (Scheme 2) were used. 2HTR is able to form dimeric and/or tetrameric intermolecular G-quadruplex structure, since it presents only two human telomeric repeats. TSG4 forms preferentially intramolecular G-quadruplex structures and can act as a substrate for telomerase elongation in a modified TRAP assay.[24] Both oligonucleotides were used in our previous works to test the ability of perylene[14] and berberine[15] derivatives to induce inter- and intramolecular G-quadruplex structures.

The two oligonucleotides were incubated with all the coronene derivatives at increasing concentrations and the formation of G-quadruplex structures was investigated by PAGE analysis, as reported in Figure 6(A–D).

Considering the mobility obtained for dimeric and tetrameric G-quadruplexes, induced by 40 μM PIPER,[14] the major electrophoresis bands were identified as single-stranded DNA (ss), dimeric (D) and monomeric (M) G-quadruplex structures. The intramolecular structure (M) corresponds to the band showing the highest mobility; its particular structure favours the running of the quadruplex in the gel matrix with respect to single-stranded DNA, although both species have the same molecular weight.[25]

It is worth noting that, in the case of TSG4, in addition to the band corresponding to M, a broad band of lower mobility appears, with increasing drug concentration. This second band could correspond to a different complex between coronene derivatives and G-quadruplex DNA, where the drug, in addition to the stacking on the terminal G-quartet, probably binds to the grooves or the loops. It could also be due to the fact that the drug can bind to DNA as an aggregate (this would increase significantly the molecular weight of the complex) or it could be associated with another different possible topology for the intramolecular G-quadruplex.

For these reasons and in order to make a comparison of the behaviour of the different drugs in the case of inter- and intramolecular G-quadruplex structures, the percentage of free DNA as a function of drug concentration was reported (Fig. 6C and D). We have chosen to report free DNA percent instead of D or M fractions, since in the case of the formation of more than one complex, this approach appears more correct. The results reported in Figure 6C and D show that the efficiency in inducing inter- and intramolecular G-quadruplex structures is dramatically different. In fact at a concentration of 20 μM, the free DNA fraction is still 60% in the case of intermolecular G-quadruplex, while it practically disappears in the case of the intramolecular G-quadruplex. At the moment, we do not have a suitable explanation for such a high selectivity between the two different G-quadruplex structures. However, it is important to remember that in the case of water-soluble perylene derivatives the G-quadruplex intramolecular structures also appeared to be favoured,[14] although to a minor extent.

2.5. Biological activity (TRAP assay)

The ability of the four coronene derivatives to inhibit human telomerase was investigated in a cell-free system by means of a modified Telomerase Repeat Amplification Protocol (TRAP) assay. Taking into account that the influence of the four molecules in inducing the intramolecular G-quadruplex appears significantly larger than in inducing intermolecular G-quadruplex structures, we have performed the TRAP assay using TSG4 (Scheme 2) as a telomerase substrate.[24] This oligonucleotide is able to fold into the intramolecular G-quadruplex at the KCl concentration used in the TRAP assay (68 mM). Nevertheless, a similar structure

2HTR: 5'-AATCCGTCGAGCAGAGTTA**GGG**TTA**GGG**TTAG-3'

TSG4: 5'-**GGG**ATT**GGG**ATT**GGG**ATT**GGG**TT-3'

Scheme 2.

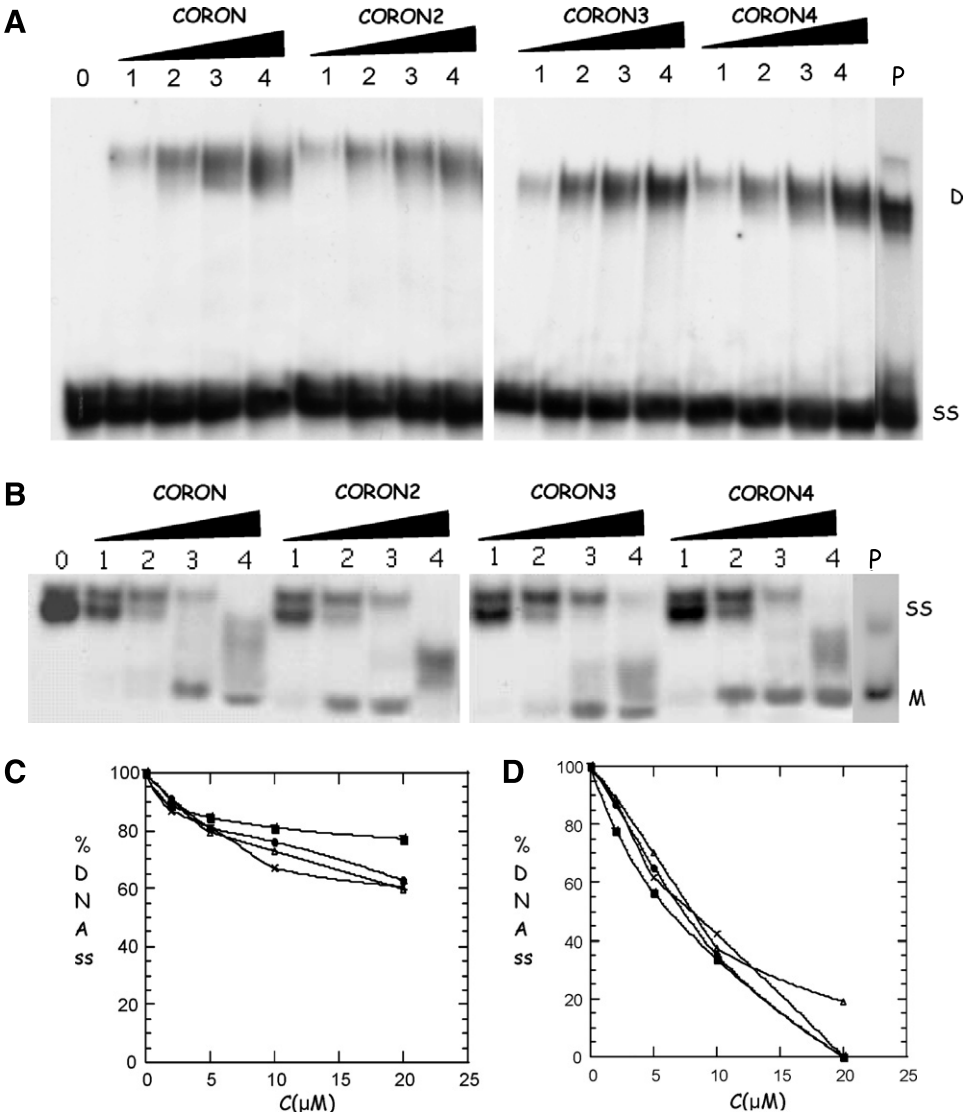

Figure 6. G-quadruplex structure formation induced by the four coronene derivatives, studied by native PAGE. (A) Typical autoradiographies obtained using 2HTR oligonucleotide (12 μM) in the presence of different drug concentrations: 2 μM (lane 1), 5 μM (lane 2), 10 μM (lane 3), 20 μM (lane 4) and with no drug (lane 0). (B) The same as in (A) but using TSG4 oligonucleotide. As standard in lane P the structures induced by PIPER at concentration 40 μM are reported. Major bands were identified as single-stranded DNA (ss), dimeric (D) and monomeric (M) G-quadruplex structures. (C–D) Percentage of single-stranded DNA in function of drug concentrations (C (μM)), for 2HTR (C) and TSG4 (D) experiments, respectively. CORON (●), CORON2 (■), CORON3 (△), CORON4 (×).

may be efficiently unfolded and extended by telomerase, unless a suitable concentration of G-quadruplex stabilizing molecules is present.[24]

The results obtained by performing the TRAP assay, in the absence and in the presence of the four coronene derivatives at 10 and 20 μM, are reported in Figure 7. At both ligand concentrations telomerase inhibition could be evaluated around 50%, but while at 10 μM a good reproducibility was observed in independent experiments (Table 2), unexpected and variable values were obtained at 20 μM. This could depend on the formation of inhomogeneous complexes between the G-quadruplex and coronene derivatives at this concentration, as suggested by the broad electrophoretic bands (Fig. 6). In fact, it is reasonable to suppose that at high ligand concentrations different binding modes to the G-quadruplex can occur, both as single ligand molecules and as aggregates. On the other hand, when the concentrations of the coronene derivatives were lowered, telomerase was not significantly inhibited (data not shown). These results seem to be in agreement with PAGE results, although it is worth noting that it is difficult to make a direct correlation between the two methods, because of the different conditions used.[14]

For these reasons, in Table 2 we considered only the percentage of telomerase inhibition obtained at 10 μM concentration of the coronene derivatives, as the optimal concentration to test telomerase inhibition by these compounds. It is worth noting that these data are quite well correlated to the relative scale of binding energies,

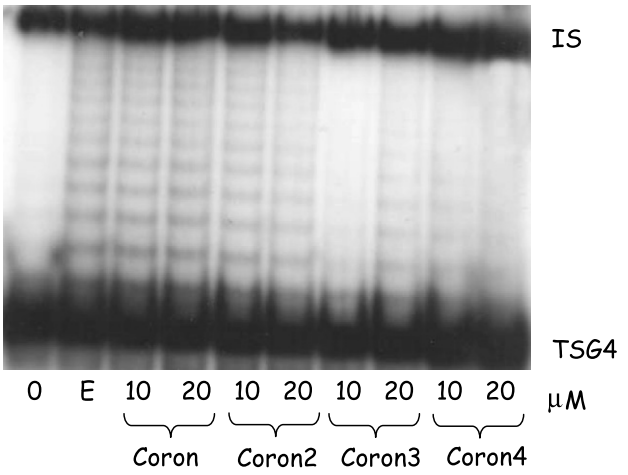

Figure 7. Inhibition of human telomerase by the four coronene derivatives by telomerase repeat amplification protocol assay (TRAP). In lane 0 cell extract was not added, in lane E no drug was added. IS is a 130 bp 'internal standard' to control the PCR amplification efficiency.

Table 2. Percentage of telomerase inhibition due to the four coronene derivatives, derived by TRAP assay, at 10 μM drug concentration

Ligand	Percentage of telomerase inhibition
CORON	38 ± 5
CORON2	44 ± 2
CORON3	66 ± 2
CORON4	52 ± 2

The values were obtained averaging the results of at least three independent experiments.

obtained by molecular modelling simulations (Table 1), although different topologies could occur for the intramolecular G-quadruplex.

3. Conclusions

In developing new telomerase inhibitors two main features have to be taken into account: the hydrophobic interactions with the G-quartet plane and the electrostatic interactions with the negative charged phosphates of the four grooves.[8] In principle, the coronene derivatives we synthesized and studied could be considered molecules with optimal features to interact with the G-quadruplex and consequently to inhibit telomerase. In fact, they show a wide aromatic core and four side chains correctly directed into the directions of the four grooves of the G-quadruplex (Fig. 4).

Our study shows that, although all the coronene derivatives are interesting inhibitors at 10 μM concentration in a cell-free system, their activity is not significantly improved with respect to perylene derivatives which we have previously studied.[14] What is the cause of this behaviour? The main factor is surely the formation of very stable stacked aggregates in water solution due to the large aromatic moiety of the molecule. The four charged chains are not able to balance the strong tendency of coronene derivatives to form aggregates in aqueous solutions (Fig. 5).

This feature represents an obstacle to the interactions with the G-quadruplex by 'threading intercalation' and suggests that the monomer concentration is important for the activity of these compounds. Further investigations are currently being carried out in our group to fully exploit these topics and to determine the binding affinities of the drugs to different DNA structures.

4. Experimental

4.1. Molecular modelling

All the experiments were performed using the InsightII package. The G-quadruplex structure used in all the simulations is the X-ray-derived monomeric structure of the 22-mer human telomeric DNA sequence AGGG $(TTAGGG)_3$ (PDB code 1KF1).[18] Ligand molecules were built using the Builder module in InsightII and their structures were energy-minimized (2000 steps, Polack-Ribiere conjugated gradient) using the Discover_3 module. Docking was performed with the Affinity Docking module of InsightII. The binding site was defined as the external 3′ G-quartet plane.[26] In the first phase 200 ligand orientations were randomly centred on the G-quadruplex structure, charges were not considered, non-bonded cutoffs were set to 8 Å and van der Waals radii to 10% of the full value. The complexes were minimized for 500 steps using Polak-Ribiere conjugate gradient method; energy tolerance and energy range were set, respectively, to 10,000 and 40 kcal/mol. In the second phase, the 75 lowest energy structures were used to perform simulated annealing. During this phase van der Waals radii were adjusted to their full values and a distance-dependent dielectric constant of 4.0 was used. Each system was again minimized for 500 steps and then molecular dynamics was performed, starting from a temperature of 800 K and cooling the system to 200 K over a period of 10 ps. The resulting structures were minimized for 2000 steps of conjugate gradient and the 25 structures with the lowest total energies were evaluated with the Analysis module of InsightII. The Docking module was used to calculate the intermolecular (binding) energy, obtained as a sum of electrostatic and van der Waals contributions, between drug and DNA.

4.2. Chemistry

All the commercial reagents and solvents were purchased from Aldrich. TLC plates (silica gel 60 F_{254}) and silica gel 60 (0.063–0.200 mm) for column chromatography were purchased from Merck. NMR spectra were observed with Varian Gemini 200 and Varian Mercury 300 instruments. ESI-MS spectra were recorded on Micromass Q-TOF MICRO spectrometer. Elemental analyses (C, H, N) were carried out on EA1110 CHNS-O (CE instruments). CORON (*N*,*N*′-bis[2-(1-piperidino)-ethyl]-5,11-bis[2-(1-piperidino)-ethyl]-coronene-2,3:8,9-tetracarboxylic diimide) was previously synthesized and characterized.[16]

4.2.1. 1,7-Dibromoperylene-3,4:9,10-tetracarboxylic dianhydride (2). The dianhydride **1** (5 g) was initially dissolved in 96% sulfuric acid (100 ml) and stirred for 2 h at room temperature. Elemental iodine (113 mg) was subsequently added and the mixture was heated. When a temperature of 80 °C was reached, elemental bromine (1.65 ml) was added dropwise. The reaction mixture was stirred at 100 °C for 4–6 h. After cooling, it was added dropwise to ice and then filtered and washed with a 5% sodium metabisulfite solution to provide a red solid (6 g), which was dried and characterized (yield: 87%). In addition to the compound **2** a small amount of the 1,6-dibromoperylene-3,4:9,10-tetracarboxylic dianhydride was also obtained. The two isomers could not be separated, so the mixture was used in the following steps without further purification.[16] ^{1}H NMR (200 MHz, D_2SO_4): δ 10.71 (d, J = 8 Hz, 2H, aromatic H), 10.04 (s, 2H, aromatic H), 9.82 (d, J = 8 Hz, 2H, aromatic H) ppm. The signals of the minor (1,6) isomer are mainly superimposed with those reported for **2**. Elemental analyses: $C_{24}H_6O_6Br_2$: Calcd C, 52.4; H, 1.1. Found: C, 51.6; H, 1.1.

4.2.2. *N*,*N*′-Bis[2-(1-piperidino)-ethyl]-1,7-dibromoperylene-3,4:9,10-tetracarboxylic diimide (PIPER-Br, 3). Six grams of compound **2** was dissolved in anhydrous *N*,*N*-dimethylacetamide (DMA, 60 ml) and 1,4-dioxane (60 ml). The commercially available 1-(2-aminoethyl)piperidine (3.6 ml) was added and the reaction mixture was stirred at 120 °C for 6 h under argon. After cooling, water was added and a red solid (6 g) was separated after filtration (yield: 71%). ^{1}H NMR (300 MHz, $CDCl_3$): δ 9.44 (d, J = 8 Hz, 2H, aromatic H), 8.89 (s, 2H, aromatic H), 8.67 (d, J = 8 Hz, 2H, aromatic H), 4.41 (t, J = 7 Hz, 4H, N_{imidic}–CH_2), 2.8–2.6 (br, 12H, $N_{piperidine}$–CH_2), 1.8–1.4 (br, 12H, $CH_{2piperidine}$) ppm. ^{13}C NMR APT (200 MHz, $CDCl_3$): δ 162.14 (C=O), 161.64 (C=O), 137.31 ($CH_{ar.}$), 132.17 ($C_{ar.}$), 132.02 ($C_{ar.}$), 129.29 ($CH_{ar.}$), 128.50 ($C_{ar.}$), 127.78 ($CH_{ar.}$), 126.28 ($C_{ar.}$), 122.55 ($C_{ar.}$), 122.12 ($C_{ar.}$), 120.18 ($C_{ar.}$), 55.74, 54.24, 37.41, 25.48, 23.81 ppm. MS (ESI) *m*/*z*: 769.1005 [(M+H)$^+$] (Calcd for $C_{38}H_{35}N_4O_4Br_2$: 769.1025).

4.2.3. *N*,*N*′-Bis[3-(dimethylamino)-propyl]-1,7-dibromoperylene-3,4:9,10-tetracarboxylic diimide (DAPER-Br, 4). Four grams of **2** was dissolved in anhydrous *N*,*N*-dimethylacetamide (DMA, 40 ml) and 1,4-dioxane (40 ml). Commercially available 3-dimethylamino-1-propylamine (2 ml) was added and the reaction mixture was stirred at 120 °C for 6 h under argon. Upon water addition, a red solid (4.4 g) was obtained and then separated by filtration (yield: 84%). ^{1}H NMR (300 MHz, $CDCl_3$): δ 9.44 (d, J = 8 Hz, 2H, aromatic H), 8.88 (s, 2H, aromatic H), 8.66 (d, J = 8 Hz, 2H, aromatic H), 4.25 (t, J = 7 Hz, 4H, N_{imidic}–CH_2), 2.44 (t, J = 7 Hz, 4H, N_{aminic}–CH_2), 2.26 (s, 12H, N_{aminic}–CH_3), 1.92 (t, J = 7 Hz, 4H, N_{imidic}–CH_2–CH_2–CH_2–N_{aminic}) ppm. ^{13}C NMR ($CDCl_3$): δ 162.64 (C=O), 162.14 (C=O), 137.80 (ar.), 132.64 (ar.), 132.51 (ar.), 129.78 (ar.), 128.99 (ar.), 128.29 (ar.), 123.07 (ar.), 122.62 (ar.), 120.67 (ar.), 126.74 (ar.), 57.23, 45.34, 39.17, 26.01. MS (ESI) *m*/*z*: 717.0752 [(M+H)$^+$] (Calcd for $C_{34}H_{31}Br_2N_4O_4$: 717.0712).

4.2.4. Synthesis of functionalized alkynes; compound 6. 3-Butyn-1-ol (**5**) was converted into its mesylate (**6**) by reaction with methanesulfonyl chloride.[27] The reagent (4.3 ml) was added dropwise at 0 °C to a mixture of anhydrous dichloromethane (80 ml), triethylamine (11 ml) and the alcohol (4 ml). The reaction mixture was then stirred for 2 h at room temperature. Successively, the organic layer was washed with water, HCl 0.5 M, saturated $NaHCO_3$ solution and saturated NaCl solution. After treatment with anhydrous Na_2SO_4, most of the solvents were evaporated under vacuum and the remainder was removed by bubbling N_2 into the liquid. 7.2 g of a pale yellow liquid was obtained (94% yield). ^{1}H NMR (200 MHz, $CDCl_3$): δ 4.25 (t, J = 7 Hz, 2H, SO–CH_2), 3.01 (s, 3H, S–CH_3), 2.62 (td, J' = 7 Hz, J'' = 3 Hz, 2H, CH≡C–CH_2–CH_2–OS), 2.06 (t, J = 3 Hz, 1H, CH≡C) ppm.

4.2.4.1. 1-(3-Butynyl)-piperidine (7). 4.5 g of mesylate **6** was stirred with piperidine (6 ml) in refluxing acetonitrile (50 ml) overnight. After cooling, dichloromethane was added and the organic layer was repeatedly washed with water. After treatment with anhydrous Na_2SO_4, most of the solvent was evaporated under vacuum and the remaining was removed by bubbling N_2 into the liquid. 2.4 g of product (**7**) was obtained, with 58% yield. ^{1}H NMR (200 MHz, $CDCl_3$): δ 2.51 (m, 2H, ≡C–CH_2), 2.4–2.2 (br, 6H, N–CH_2), 1.91 (t, J = 3Hz, 1H, C≡C–H), 1.52 (m, 4H, $CH_{2piperidine}$), 1.38 (m, 2H, $CH_{2piperidine}$) ppm. ^{13}C NMR ($CDCl_3$): δ 82.92 (≡C), 68.70 (≡CH), 57.72, 54.07, 25.80, 24.16, 16.54 ppm.

4.2.4.2. 1-(3-Butynyl)-4-methyl-piperazine (8). Three grams of mesylate **6** was stirred with *N*-methyl-piperazine (4.5 ml) in refluxing absolute ethanol overnight. After cooling, dichloromethane was added and the organic layer was washed one time with saturated NaCl solution. The product was purified by column chromatography ($CHCl_3$/MeOH 100:0, 90:10) and 2.8 g of product was obtained, with 91% yield. ^{1}H NMR (200 MHz, $CDCl_3$): δ 2.6–2.3 (br, 12H), 2.23 (s, 3H, N–CH_3), 1.93 (t, J = 3 Hz, 1H, CH≡C) ppm. ^{13}C NMR ($CDCl_3$): δ 82.41 (≡C), 68.87 (≡CH), 56.71, 54.73, 52.55, 45.75, 16.51 ppm.

4.2.5. Synthesis of the intermediate compounds 9, 10 and 11. Starting from compound **3** (PIPER-Br) or **4** (DAPER-Br), intermediate compounds **9**, **10** and **11** were obtained by replacement of bromine atoms with the functionalized alkynes **7** and **8**. The starting compound was dissolved in anhydrous THF and triethylamine; then CuI and $Pd(PPh_3)_4$were added. After bubbling argon, the reaction mixture was heated at 80 °C with stirring and the desired alkyne was added dropwise. The mixture was then stirred at 80 °C overnight in an argon atmosphere. After cooling, diluted HCl was added and the product was extracted with dichloromethane, after neutralization with 2 M NaOH. The organic layer was washed with water until the aqueous layer was neutral. The crude product was purified by column chromatography on a silica gel ($CHCl_3$/MeOH 100:0, 95:5, 9:1, 8:2, 7:3). Since partial cyclization can occur at this stage, the complete separation of the

different products and a full characterization were not possible. The fractions obtained by chromatography showing a suitable aromatic pattern in the ^{1}H NMR spectra were collected and the mixture was used in the following cyclization step.

4.2.5.1. Compound 9. According to the procedure described above, 2.7 g of **3**, 2 g of **8**, 386 mg of $Pd(PPh_3)_4$, 65 mg of CuI, 70 ml of anhydrous THF and 70 ml of anhydrous Et_3N were used to obtain 1 g of intermediate compound **9**.

4.2.5.2. Compound 10. According to the procedure described above, 2.2 g of **4**, 1.9 g of **8**, 353 mg of $Pd(PPh_3)_4$, 58 mg of CuI, 60 ml of anhydrous THF and 60 ml of anhydrous Et_3N were used to obtain 650 mg of intermediate compound **10**.

4.2.5.3. Compound 11. According to the procedure described above, 1.5 g of **4**, 1.14 g of **7**, 240 mg of $Pd(PPh_3)_4$, 39 mg of CuI, 30 ml of anhydrous THF and 30 ml of anhydrous Et_3N were used to obtain 140 mg of intermediate compound **11**.

4.2.6. *N*,*N*′-Bis[2-(1-piperidino)-ethyl]-5,11-bis[2-(4- methyl-1-piperazino)-ethyl]-coronene-2,3:8,9-tetracarboxylic diimide (CORON2, 12). One gram of **9** was dissolved in 100 ml of toluene and 0.34 ml of 1,8-diaza-bicyclo[5.4.0]undec-7-ene (DBU) was added. The reaction mixture was refluxed with stirring under argon for 20 h. After cooling, dichloromethane was added and the organic layer was extracted with water until the aqueous layer was neutral. The crude product was purified by column chromatography on a silica gel ($CHCl_3$/MeOH 100:0, 98:2, 95:5, 9:1, 8:2, 7:3) to give 230 mg (7% yield) of compound **12**. It was then crystallized by dissolving it in 0.2 M HCl and precipitating the respective hydrochloride by adding acetone. One hundred and forty milligrams of hydrochloride was obtained starting from 170 mg of basic compound (65% yield). ^{1}H NMR (300 MHz, $CDCl_3$): δ 9.38 (s[†]), 9.33 (s, 2H, aromatic H), 9.13 (s, 2H, aromatic H), 9.08 (s[†]), 8.36 (s, 2H, aromatic H), 4.46 (t, J = 7 Hz, 4H, N_{imidic}–CH_2), 3.73 (t, J = 7 Hz, 4H, $C_{ar.}$–CH_2), 3.0–2.6 (br, 32H, N–CH_2), 2.41 (s, 6H, N–CH_3) 1.72 (br, 8H, $CH_{2piperidine}$), 1.54 (br, 4H, $CH_{2piperidine}$) ppm. ^{13}C NMR (CDCl3): d 163.93 (C═O), 163.76 (C═O), 138.58 (ar.), 128.98 (ar.), 128.21(ar.), 127.91 (ar.), 127.60 (ar.), 124.98 (ar.), 121.57 (ar.),121.08 (ar.), 120.61 (ar.), 120.34 (ar.), 120.34 (ar.), 118.90 (ar.), 59.31, 56.52, 55.18, 54.90, 53.32, 46.05, 38.11, 30.96, 26.06, 24.41 ppm. MS (ESI) *m*/*z*: 913.5139 [(M+H)$^+$] (Calcd for $C_{56}H_{65}N_8O_4$: 913.5129).

4.2.7. *N*,*N*′-Bis[3-(dimethylamino)-propyl]-5,11-bis[2-(4-methyl-1-piperazino)-ethyl]-coronene-2,3:8,9-tetracarboxylic diimide (CORON3, 13). CORON3 (**13**) was obtained, as described for **12**, by reaction of compound **10** (650 mg), dissolved in 50 ml of toluene, with 0.24 ml of DBU. The reaction mixture was refluxed with stirring under argon for 20 h. After cooling, dichloromethane was added and the organic layer was extracted with water until the aqueous layer was neutral. The crude product was purified by column chromatography on a silica gel ($CHCl_3$/MeOH 100:0, 98:2, 95:5, 9:1, 8:2, 7:3) to give 260 mg (10% yield) of compound **13**. This was then crystallized by dissolving 200 mg in 0.2 M HCl and precipitating the respective hydrochloride (180 mg) with acetone (72% yield). ^{1}H NMR (300 MHz, $CDCl_3$): δ 9. 01 (s[†]), 8.89 (s, 2H, aromatic H), 8.73 (s, 2H, aromatic H), 8.59 (s[†]), 8.02 (s, 2H, aromatic H), 8.00 (s[†]), 4.37 (br, 4H, N_{imidic}–CH_2), 3.48 (br, 4H, $C_{ar.}$–CH_2), 2.9–2.1 (br) ppm. ^{13}C NMR ($CDCl_3$): δ 163.42 (C═O), 163.33 (C═O), 138.25 (ar.), 128.35 (ar.), 127.61(ar.), 127.28 (ar.), 127.03 (ar.), 124.28 (ar.), 120.68 (ar.),120.39 (ar.), 120.07 (ar.), 119.78 (ar.), 119.50 (ar.), 118.04 (ar.), 58.93, 57.31, 55.22, 53.37, 46.07, 45.35, 39.34, 30.55, 26.10 ppm. MS (ESI) *m*/*z*: 861.4794 [(M+H)$^+$] (Calcd for $C_{52}H_{61}N_8O_4$: 861.4816).

4.2.8. *N*,*N*′-Bis[3-(dimethylamino)-propyl]-5,11-bis[2-(1-piperidino)-ethyl]-coronene-2,3:8,9-tetracarboxylic diimide (CORON4, 14). One hundred and forty milligrams of compound **10** was dissolved in 30 ml of toluene and 0.06 ml of 1,8-diaza-bicyclo[5.4.0]undec-7-ene (DBU) was added. The reaction mixture was refluxed with stirring under argon for 20 h. After cooling, dichloromethane was added and the organic layer was extracted with water until the aqueous layer was neutral. The crude product (125 mg, 10% yield) was pure enough to be precipitated as a hydrochloride by dissolving it in 0.2 M HCl and adding acetone: 78 mg was obtained, with 53% yield. ^{1}H NMR (200 MHz, $CDCl_3$): δ 9.36 (s[†]) 9.30 (s, 2H, aromatic H), 9.08 (s, 2H, aromatic H), 9.00 (s[†]), 8.32 (s, 2H, aromatic H), 8.30 (s[†]), 4.50 (br, 4H, N_{imidic}–CH_2), 3.72 (br, 4H, $C_{ar.}$–CH_2), 2.95 (br, 4H, N–CH_2), 2.8–2.5 (br, 12H, N–CH_2), 2.37 (s, 12H, CH_3–N), 1.78 (br, 12H, CH_2–CH_2–N_{aminic}), 1.58 (br, 4H, $CH_{2piperidine}$) ppm. ^{13}C NMR ($CDCl_3$): δ 163.67 (C═O), 163.57 (C═O), 138.78 (ar.), 128.55 (ar.), 127.92 (ar.), 127.62 (ar.), 127.37 (ar.), 124.67 (ar.), 121.15 (ar.),120.70 (ar.), 120.30 (ar.), 120.06 (ar.), 119.94 (ar.), 118.51 (ar.), 60.13, 57.46, 54.80, 45.48, 39.45, 30.76, 29.64, 26.22, 24.50 ppm. MS (ESI) *m*/*z*: 831.4552 [(M+H)$^+$] (Calcd for $C_{52}H_{59}N_6O_4$: 831.4598).

4.3. UV–vis absorption spectroscopy

UV–vis absorption spectra were performed using a JASCO V-530 spectrophotometer. They were registered between 300 and 600 nm in quartz cuvettes. Four hundred micromolar drug stocks, prepared by dissolving the hydrochlorides in DMSO, were diluted to observe spectra in aqueous solution (10 mM MES-50 mM KCl buffer, pH 6.5) and in DMSO.

4.4. Polyacrylamide gel electrophoresis (PAGE)

Previously radio-labelled 2HTR and TSG4 oligonucleotides (whose sequences are reported in Scheme 2) were heated at 95 °C for 10 min and quickly cooled in ice, at a concentration of 12 μM. Then they were incubated

[†] Aromatic ^{1}H NMR singlets due to the minor 5,10-isomer derived from the 1,6-dibromoperylene anhydride. Integration of the signals shows that the ratio of the two isomers is about 6:1.

for 2 h at 30 °C in MES–KCl buffer (10 mM MES, pH 6,5, 50 mM KCl for 2HTR and 5 mM KCl for TSG4) in the presence of different drug concentrations and with no drug. Complexes and structures formed after incubation were studied by native PAGE (15% polyacrylamide gel, TBE 0.5X, KCl 20 mM, run overnight at 4 °C).

In all electrophoresis runs, the G-quadruplex induction by PIPER (40 μM) was also reported as a useful standard to assign the electrophoresis bands to different DNA conformations. Major bands were so identified as single-stranded DNA (ss), dimeric (D), tetrameric (T) and monomeric (M) G-quadruplex structures.[14]

4.5. Telomerase repeat amplification protocol (TRAP) assay

The reaction mixture for assaying inhibition of human telomerase (50 μl) contains 50 μM dNTPs, 0,4 μM TSG4 primer and 1 μl of cell extract (prepared from 10^7 cultured human Neuroblastoma cells) in TRAP buffer (20 mM Tris–HCl, pH 8.3, 1.5 mM $MgCl_2$, 68 mM KCl, 0.05% Tween 20 and 1 mM EGTA). In each sample, coronene derivatives were added at different concentrations and incubated for 2 h at 30 °C, before addition of the cell extract. After 30 min of incubation at 30 °C, the samples were purified by phenol/chloroform extraction. ^{32}P radiolabelled TSG4 (0,14 μM), 0,4 μM CXext primer and 2U *Taq* DNA polymerase (Eppendorf) were added and 30 PCR cycles were performed (94 °C 10′, 92 °C 30″, 54 °C 30″, 72 °C 5′30″). Finally, the samples were loaded on a nondenaturing 12% polyacrylamide gel. Samples with no drug and with no cell extract were references. A 130 bp 'internal standard' (IS) was used to evaluate PCR amplification efficiency.[28]

Acknowledgments

This research has been financially supported by MIUR-FIRB 2001, MIUR-COFIN 2005 and by Istituto Pasteur-Fondazione Cenci Bolognetti. Thanks are due to S. Nasi and D. Annibali for having provided the human Neuroblastoma cells for telomerase extract, to S. Bacchetti for the protocol for telomerase extraction, to Dr. Luigi Rossetti for helpful discussion and to Dr. Christoph Schultes for help in the final revision of the manuscript. A financial contribution by ARPA-Lazio funding for a research fellowship to C. Mauriello is gratefully acknowledged.

Supplementary data

Supplementary data associated with this article can be found, in the online version, at doi:10.1016/j.bmc.2006.11.032.

References and notes

1. Neidle, S.; Parkinson, G. N. *Curr. Opin. Struct. Biol.* **2003**, *13*, 275.
2. Rhodes, D.; Giraldo, R. *Curr. Opin. Struct. Biol.* **1995**, *5*, 311.
3. Neidle, S.; Parkinson, G. *Nat. Rev. Drug Discov.* **2002**, *1*, 383.
4. Giraldo, R.; Suzuki, M.; Chapman, L.; Rhodes, D. *Proc. Natl. Acad. Sci. U.S.A.* **1994**, *91*, 7658.
5. Han, H.; Bennett, R. J.; Hurley, L. H. *Biochemistry* **2000**, *39*, 9311.
6. Schaffitzel, C.; Berger, I.; Postberg, J.; Hanes, J.; Lipps, H. J.; Pluckthun, A. *Proc. Natl. Acad. Sci. U.S.A.* **2001**, *98*, 8572.
7. Paeschke, K.; Simonsson, T.; Postberg, J.; Rhodes, D.; Lipps, H. J. *Nat. Struct. Mol. Biol.* **2005**, *12*, 847.
8. Incles, C. M.; Schultes, C. M.; Neidle, S. *Curr. Opin. Invest. Drugs* **2003**, *4*, 675.
9. Shay, J. W.; Wright, W. E. *Cancer Cell* **2002**, *2*, 257.
10. Kelland, L. R. *Eur. J. Cancer* **2005**, *41*, 971.
11. Moore, M. J.; Schultes, C. M.; Cuesta, J.; Cuenca, F.; Gunaratnam, M.; Tanious, F. A.; Wilson, W. D.; Neidle, S. *J. Med. Chem.* **2006**, *49*, 582.
12. Gomez, D.; Aouali, N.; Renaud, A.; Douarre, C.; Shin-Ya, K.; Tazi, J.; Martinez, S.; Trentesaux, C.; Morjani, H.; Riou, J. F. *Cancer Res.* **2003**, *63*, 6149.
13. Seenisamy, J.; Bashyam, S.; Gokhale, V.; Vankayalapati, H.; Sun, D.; Siddiqui-Jain, A.; Streiner, N.; Shin-Ya, K.; White, E.; Wilson, W. D.; Hurley, L. H. *J. Am. Chem. Soc.* **2005**, *127*, 2944.
14. (a) Rossetti, L.; Franceschin, M.; Bianco, A.; Ortaggi, G.; Savino, M. *Bioorg. Med. Chem. Lett.* **2002**, *12*, 2527; (b) Rossetti, L.; Franceschin, M.; Schirripa, S.; Bianco, A.; Ortaggi, G.; Savino, M. *Bioorg. Med. Chem. Lett.* **2005**, *15*, 413.
15. Franceschin, M.; Rossetti, L.; D'Ambrosio, A.; Schirripa, S.; Bianco, A.; Ortaggi, G.; Savino, M.; Schultes, C.; Neidle, S. *Bioorg. Med. Chem. Lett.* **2006**, *16*, 1707.
16. Franceschin, M.; Alvino, A.; Ortaggi, G.; Bianco, A. *Tetrahedron Lett.* **2004**, *45*, 9015.
17. Han, H.; Cliff, C. L.; Hurley, L. H. *Biochemistry* **1999**, *38*, 6981.
18. Parkinson, G. N.; Lee, M. P.; Neidle, S. *Nature* **2002**, *417*, 876.
19. Fedoroff, O. Y.; Salazar, M.; Han, H.; Chemeris, V. V.; Kerwin, S. M.; Hurley, L. H. *Biochemistry* **1998**, *37*, 12367.
20. (a) Ambrus, A.; Chen, D.; Dai, J.; Bialis, T.; Jones, R. A.; Yang, D. *Nucleic Acids Res.* **2006**, *34*, 2723;; (b) Luu, K. N.; Phan, A. T.; Kuryavyi, V.; Lacroix, L.; Patel, D. J. *J. Am. Chem. Soc.* **2006**, *128*, 9963.
21. (a) Moore, M. J.; Cuenca, F.; Searcey, M.; Neidle, S. *Org. Biomol. Chem.* **2006**, *4*, 3479;; (b) Reed, J. E.; Arnal, A. A.; Neidle, S.; Vilar, R. *J. Am. Chem. Soc.* **2006**, *128*, 5992.
22. (a) Rohr, U.; Kohl, C.; Mullen, K.; van de Craats, A.; Warman, J. *J. Mater. Chem.* **2001**, *11*, 1789; (b) Rohr, U.; Schlichting, P.; Bohm, A.; Gross, M.; Meerholz, K.; Brauchle, C.; Mullen, K. *Angew. Chem., Int. Ed.* **1998**, *37*, 1434.
23. Sonogashira, K.; Tohda, Y.; Hagihara, N. *Tetrahedron Lett.* **1975**, 4467.
24. Gomez, D.; Mergny, J. L.; Riou, J. F. *Cancer Res.* **2002**, *62*, 3365.
25. (a) Henderson, E.; Hardin, C. C.; Walk, S. K.; Tinoco, I., Jr.; Blackburn, E. H. *Cell* **1987**, *51*, 899; (b) Williamson, J. R.; Raghuraman, M. K.; Cech, T. R. *Cell* **1989**, *59*, 871.
26. Harrison, R. J.; Cuesta, J.; Chessari, G.; Read, M. A.; Basra, S. K.; Reszka, A. P.; Morrell, J.; Gowan, S. M.; Incles, C. M.; Tanious, F. A.; Wilson, W. D.; Kelland, L. R.; Neidle, S. *J. Med. Chem.* **2003**, *46*, 4463.
27. Crossland, R. K.; Servis, K. L. *J. Org. Chem.* **1970**, *35*, 3195.
28. Gan, Y.; Lu, J.; Johnson, A.; Wientjes, M. G.; Schuller, D. E.; Au, J. L. *Pharm. Res.* **2001**, *18*, 488.